Geomorphology 115 (2010) 188–193

Contents lists available at ScienceDirect

Geomorphology

journal homepage: www.elsevier.com/locate/geomorph

Subaerial and subaqueous dynamics of coastal rockfalls

Fabio Vittorio De Blasio [a,*], Paolo Mazzanti [b]

[a] Department of Geosciences, University of Oslo, P.O. Box 1047 Blindern, N-0316 Oslo, Norway
[b] Department of Earth Sciences, University of Rome "Sapienza", P.le Aldo Moro 5, 00185, Roma, Italy

ARTICLE INFO

Article history:
Received 30 April 2009
Received in revised form 1 September 2009
Accepted 3 September 2009
Available online 12 September 2009

Keywords:
Rockfalls
Coastal rockfalls
Mixed Rockfall (MRF)
Scilla-Palmi coast
Lake Albano

ABSTRACT

In spite of the hazard represented by rockfalls in coastal areas, few investigators have studied the movement of rocks falling in water. This work describes a model for the propagations of coastal rockfalls, i.e., blocks detaching from a subaerial cliff, propagating initially in air, impacting against the water surface, and finally coming to rest in the water basin. Application of the model to two real cases in Italy shows a satisfactory agreement between the predicted rockfall run-out and the field data. Some scattering observed in the data is explained as the consequence of different heights of the source area. It is shown that largest boulders usually reach a longer distance. However, the schematic shape for blocks adopted in the model likely results in a much more regular behaviour compared to reality.

1. Introduction

Landslides starting subaerially and ending in a water basin represent a peculiar class of mass wasting where the characters of subaerial and subaqueous movements are both important. Described cases are limited but relatively well studied. They include subaerial slides plunging into fjords (Longva et al., 2003), lakes (Mazzanti et al., 2007; Bozzano et al., 2009) or the sea (Chiocci et al., 2008; Bozzano et al., 2008; Mazzanti, 2008). The mechanical problems posed by this kind of events are fairly novel and have relevant applications. The impact with water is capable of generating particularly high tsunamis compared to entirely subaqueous slides (Miller, 1960; Harbitz et al., 1993; Mazzanti, 2008). Along this research line, the present paper addresses a smaller-scale problem, i.e., the dynamics of isolated blocks detaching from a subaerial cliff, impacting against a water surface, and finally coming to rest in the water basin.

Due to the relevant threat represented by rockfalls in mountain areas, many models have been developed that simulate rocks falling subaerially (Bozzolo and Pamini, 1986; Pfeiffer and Bowen, 1989; Giani, 1992; Evans and Hungr, 1993; Azzoni and De Freitas, 1995; Jones et al., 2000; Guzzetti et al., 2002; Dorren, 2003). Studies addressing the rockfall hazard in open sea structures or ships have been restricted to the subaerial trajectory only (Crosta et al., 2007). Surprisingly, few studies have considered the rockfall problem when the end point of blocks occurs in water, accounting also for the submerged trajectory of the block. A better understanding of the subaqueous dynamics is highly desirable at least from three viewpoints. Firstly, the subaqueous deposits from rockfalls may reach in some cases relevant volumes; this makes the problem of the subaqueous blocks distribution of interest for sedimentology and geomorphology. Secondly, the documented cases of rockfalls in the sea, fjords or lakes may put subaqueous structures at risk (Beranger et al., 1998). Finally, the dynamics of a block moving in water and the impact against the water surface are motivating problems in themselves, relevant for geophysics and fluid mechanics. Turmel and Locat (2007) have preliminarily estimated the forces acting on a block moving in water without calculating the block trajectories. These authors focused only on the subaqueous part, thus ignoring the impact with water.

In this paper we present a model for rockfalls starting subaerially, plunging into a water basin, and then moving in water. For brevity we will call Mixed Rockfall (MRF) the event comprised between the detachment of the block on land to the final stop in the water basin. There are many physical issues involved in the study of MRFs. In addition to the propagation of the rock in air, addressed in the mentioned investigations, in the watery phase both lift and drag forces become important. The impact with the bottom and the rolling friction along the subaqueous floor may also disclose a different character from the subaerial case due to the different types of sediment and the saturation conditions of the soil. Moreover, the impact with the water surface will deprive a block of part of its kinetic energy.

Specifically, we calculate the forces acting on blocks of various sizes and integrate the equation of motion to calculate their velocity and trajectory. We predict trajectories and run-outs for two actual cases: the Lake Albano in central Italy, and the sea offshore Scilla in southern Italy.

* Corresponding author.
E-mail address: fvblasio@geologi.uio.no (F.V. De Blasio).

0169-555X/$ – see front matter © 2009 Elsevier B.V. All rights reserved.
doi:10.1016/j.geomorph.2009.09.024

2. Mixed Rockfall model: theory

In this section we sketch the basic theory of the model. The forces controlling the dynamics of a block can be listed as follows: 1) the gravity force; 2) the Archimedean buoyancy; 3) the drag force parallel but opposite to the block velocity due to water and air resistance; 4) the drag torque exerted against the block rotation; 5) the lift force perpendicular to block velocity and acting upwards if the block moves from left to right and spins anticlockwise; 6) the impact force when the block hits the water surface; 7) the impact force against the terrain, both in subaerial and subaqueous conditions; 8) the rolling friction force when the block rolls on the terrain, and 9) the sliding friction force when the block slides on the terrain. Of these forces, 2, 3, 4 and 5 are important only in the subaqueous part of the trajectory; 6 is significant only at the boundary; and 7, 8 and 9 are formally identical in the subaerial and subaqueous parts of the trajectory, albeit with different values of the coefficients. Blocks are considered as cylinders of radius R.

2.1. Block propagation far from the phase boundaries

Far from the terrain and the water surface, the equation of motion for the x and y components of a block in free fall can be written in the form

$$\left(1+\alpha_j\frac{\rho_j}{\rho_S}\right)\frac{dv}{dt} = -g\frac{\Delta\rho_j}{\rho_S} - \frac{2}{\pi D}C_{D,j}\frac{\rho_j}{\rho_S}U^2 e_y + 4\pi C_{L,j}\frac{\rho_j}{\rho_S}\Omega U e_x \quad (1)$$

$$\left(1+\alpha_j\frac{\rho_j}{\rho_S}\right)\frac{du}{dt} = -\frac{2}{\pi D}C_{D,j}\frac{\rho_j}{\rho_S}U^2 e_x + 4\pi C_{L,j}\frac{\rho_j}{\rho_S}\Omega U e_y \quad (2)$$

where α_j, u, v on the left hand side represent respectively the effective mass coefficient and the x and y components of the velocity, whereas the quantities g, ρ_S, $\Delta\rho$, ρ_j and D on the right hand side are the gravity acceleration, the density of the block, the density difference between the block and the medium, the density of the medium, and the block diameter. The index j is equal to one for air and two for water; each parameter indexed with j may so acquire different values in the two environments. Finally, C_D and C_L are the drag and lift coefficients, $U=(u^2+v^2)^{1/2}$ is the magnitude of the velocity, Ω is the angular velocity, and e_x and e_y are unit vectors along x and y.

In the absence of collision with the boundaries, the angular velocity of the block varies due to the skin drag with the medium as

$$\frac{d\Omega}{dt} = -\frac{\rho_j}{\rho_S}C_{SKIN}\Omega^2 \quad (3)$$

where C_{SKIN} is the drag skin friction coefficient.

2.2. Impact with water

The impact force with water (F_{IMP}) is written as

$$F_{IMP} = \frac{1}{2}\rho_j C_{IMP} U_\perp^2 S \quad (4)$$

where C_{IMP} and $U_\perp$ are respectively the impact coefficient and the component of block velocity perpendicular to the water surface, whereas S is the cross area of the cylinder. The parameter C_{IMP} is parameterized from the Shiffman Spencer model (Shiffman and Spencer, 1945); following validation by Moghisi and Squire (1981), it is written as $C_{IMP}=a_1 b^{1/2}-a_2 b$ with $a_1=5.22$, $a_2=5.42$. The dimensionless quotient $b=(y-W)/R$ is the ratio between the wetted depth $y-W$ and the cylinder radius, where y and W are the height of the cylinder centre and the water level, respectively. Although this relationship strictly holds for spheres, we do not expect significant differences when the aspect ratio of the cylinder is close to unity, as assumed here.

2.3. Impact with the terrain

The collision with the terrain is modelled as follows. We define two coefficients of restitution $\varepsilon_{\|,j}$, $\varepsilon_{\perp,j}$ respectively parallel and perpendicular to impact (Goldsmith, 1960). When the block hits the slope with a certain velocity $u_\|$, $u_\perp$ (velocity components parallel and perpendicular to slope, more convenient for the analysis), angular velocity Ω and angle γ, it is bounced back with new values $u'_\|$, $u'_\perp$ Ω' and γ'. These are calculated from momentum and angular momentum conservation assuming lack of slippage at the base of the block (Goldsmith, 1960)

$$u'_\| = \frac{2}{3}[(1+\varepsilon_{\|,j}/2)u_{p,j} + R\Omega(1-\varepsilon_{\|,j})/2] \quad (5)$$

$$u'_\perp = -\varepsilon_{\perp,j}u_\perp \quad (6)$$

$$\Omega' = \frac{2}{3}[(1-\varepsilon_{\|,j})u_{\|,j}/R + \Omega(1/2+\varepsilon_{\|,j})] \quad (7)$$

where we consider positive the angular velocity of a block rotating clockwise. In deriving the equations, use has been made of the expression for the moment of inertia I of a cylinder,

$$I = MR^2/2 \quad (8)$$

where M is the cylinder mass.

2.4. Rolling

We assume that the block starts rolling when, after a bounce with the ground, it reaches a distance from the ground less than a definite length representing ground asperities (e.g. grass or mud in the subaerial and subaqueous environment respectively). When the cylinder is rolling, its equation of motion becomes

$$\left(1+\alpha_j\frac{\rho_j}{\rho_S}\right)\frac{du_\|}{dt} = g\frac{\Delta\rho}{\rho_S}(\sin\beta-\mu_{roll,j}\cos\beta) - \frac{2}{\pi D}C_{D,j}\frac{\rho_M u_p^2}{\rho_S} - 4\pi C_{L,j}\frac{\rho_j}{\rho_S}\Omega U\mu_{roll,j}\cos\beta \quad (9)$$

where $\mu_{roll,j}$ is the rolling friction coefficient. Because no sliding is assumed during rolling, the angular and parallel velocities are no more independent, but are linked by the equation $u_\|=\Omega R$. Due to the assumption of cylindrical shape for blocks, in the present two-dimensional model the sole variable depending on the size of the block is the radius. To compare our simulations with field data we introduce the aspect ratio of the cylinder and assume cylinder length is equal to twice the cylinder diameter.

A schematic view of the physical processes described above is reported in Fig. 1.

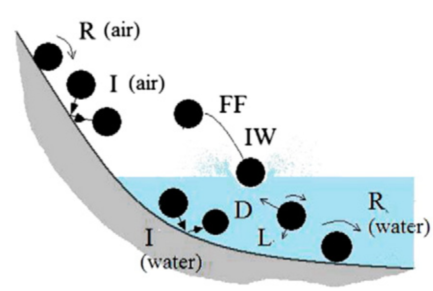

Fig. 1. Schematic view of the most important physical processes taking place during the block propagation in subaerial and subaqueous environments. I: impact with the terrain. IW: impact with water. D: drag force. L: lift force. FF: free fall. R: rolling.

3. Simulation of real cases and discussion

In connection to recent research on coastal landslides (Mazzanti, 2008), we analysed two cases of MRFs: at the Lake Albano and the offshore of Scilla, both in Italy. Sonar multibeam bathymetries with a few-centimetre resolution were collected in the frame of this research that allowed identifying several blocks larger than 10 m^3 in both the lake and sea floor. In the two investigated cases, these blocks were originated by subaerial rock scarps. Figs. 2a and b show the maps of the Scilla and Albano respectively with some of the blocks indicated with arrows. The identification of subaerial source areas and submarine (sub-lake) final locations of blocks is a key requirement

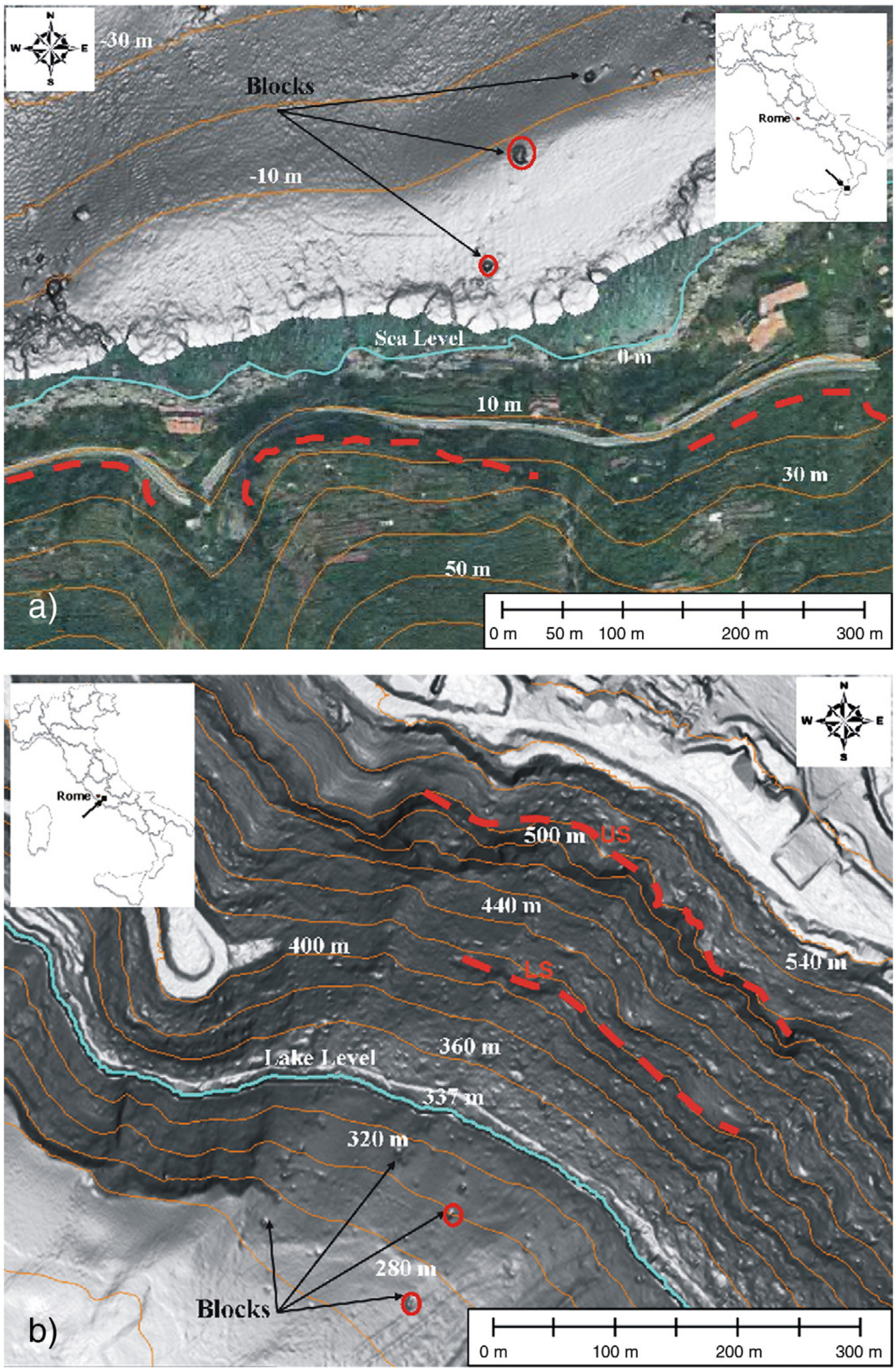

Fig. 2. Study areas. a) Aerial photo and sonar multibeam bathymetry of the coastal sector between Marina San Gregorio and Scilla (RC, Italy). Red dashed lines identify subaerial rockfall scarps, and white arrows mark submarine blocks detached from subaerial scarps. b) Combined subaerial–subaqueous shaded relief of the N–E slope of Lake Albano (Rome, Italy). Red dashed lines identify subaerial rockfall scarps (US = Upper Scarp; LS = Lower Scarp); black arrows mark some subaqueous blocks coming from subaerial scarps. The blocks used for comparison with our simulations are highlighted with circles.

Table 1
Parameters used in the calculations for both Scilla and Albano.

	α_j	C_D	C_L	C_{SKIN}	μ_{roll}	ε_p	$\varepsilon_\perp$	ρ_S (kg m^{-3})	ρ_j (kg m^{-3})
Subaerial	0.5	0.6	0.4	0.01	0.4	0.4	0.7 for Scilla; 0.8 for Albano	2300	1
Subaqueous	0.5	0.6	0.4	0.01	Subaerial rolling never occurs in the calculations	0.4	0.2 for Scilla; 0.3 for Albano	2300	1000

The symbols of the different parameters are explained in the text. Note that the perpendicular coefficients of restitution are different for Scilla and Albano.

for back calculating their trajectory and propagation. Since the resolution of the DTLM (Digital Terrain and Lacustrine Model) and DTMM (Digital Terrain and Marine Model) is finer than the size of the largest blocks, a smoothing of 5 m is applied to the terrain prior to calculations.

Whereas for the subaerial trajectory we use rather standard parameters for the restitution coefficients and rolling friction (Giani, 1992), data for a block moving underwater are more insecure. A first difference may arise from the capability of water to viscously dampen the impact between stiff surfaces (Clift et al., 1978) which is quantified by the Stokes number $St \approx \rho_S\, u_\perp\, R/8\mu$, where μ is water viscosity. At low Stokes numbers, the coefficient of restitution is substantially smaller under water than in air (Joseph et al., 2001; Gondret et al., 2002; Turmel and Locat, 2007). Stokes numbers are, however, expected to be very large ($St \gg 10^4$) so that no significant difference is expected between the subaerial and subaqueous situation if the colliding surface has the same properties.

However, the mechanical properties of the subaerial and subaqueous terrain surfaces are probably very different due to the dissimilar depositional conditions. The upper underwater layers at Lake Albano and Scilla are covered by a veneer of muddy sediments and sandy soil, respectively (Mazzanti, 2008). These soft layers likely result in small subaqueous coefficient of restitution to an extent that is difficult to quantify. Likewise, the coefficient of rolling friction must be comparatively higher than in the subaerial environment. Even for the subaerial environment there is no theory to predict the coefficient of rolling friction on a granular material. Therefore it is common practice to directly measure it by on site tests and experiments (see e.g. Azzoni and De Freitas, 1995). Typical values for unconsolidated terrain are in the range 0.50–0.75 (Giani, 1992; Azzoni and De Freitas, 1995; De Blasio and Sæter, 2009) whereas 0.4 is more appropriate for hard rock. The fluid-dynamical parameters are chosen as follows (e.g., Hughes and Brighton, 1967). The drag coefficient of 0.6 corresponds to a cylinder with diameter comparable or slightly shorter that its length, in motion at high Reynolds numbers. A practical value for the lift coefficient is provided by the Kutta–Joukowski theorem for a rotating cylinder (e.g., Hughes and Brighton, 1967). Considering the irregular shape of a real block, we have reduced this coefficient to a value $C_L = 1/2$. Although more secure data would be desirable for irregular blocks, we believe all the parameters are acceptable to a first approximation. The complete dataset of parameters and coefficients used in the simulation is reported in Table 1.

Fig. 3 shows the calculated trajectory of a 4 m radius block falling along the Scilla slope. The block initially bounces with progressively longer leaps before splashing against the water surface. In water, the velocity of the block is progressively reduced; shortly after impact, the lift force on the spinning block bends the trajectory bottom-ward. In the subaqueous environment usually one or two single bounces take place, after which the rolling regime ensues. The stoppage of the block occurs during the rolling phase and for real blocks it is facilitated by shape irregularities. A block with the shape of a regular polyhedron would stop when the kinetic energy becomes equal to the potential energy necessary to lift the centre of mass on one of its edges. In the calculations we imposed a hexagonal shape to the block as a criterion for stoppage. Whereas the subaerial trajectory can be compared to two-dimensional rockfall calculations obtained with other numerical models (Bozzolo and Pamini, 1986; Pfeiffer and Bowen, 1989; Giani, 1992; Evans and Hungr, 1993; Azzoni and De Freitas, 1995; Jones et al., 2000), the submerged trajectory appears different owing to the effect of the water. The lack of previous calculations of this kind in the subaqueous environment makes a similar comparison impossible for the submerged trajectories.

Having obtained a reasonable value for the run-out of the 4 m block, we calculated the trajectory of some smaller blocks. The arrows in Fig. 3 specify the final positions of real blocks with their estimated volume; the location of some other computed blocks is also shown as grey circles with the value of the radius used in the calculation. A trend towards a decrease of the run-out for smaller blocks is clearly predicted by the model, and appears to be in line with the field observations. Fig. 3 also shows the velocity of the block's centre of mass, which exhibits some gaps in correspondence of the impacts with the terrain. The block usually ends its motion underwater during the rolling phase.

Fig. 4 shows the results for the Lake Albano rockfalls, characterized by higher block leaps, greater velocities, and longer run-out compared to the Scilla blocks. The velocity of impact with water (>40 m s^{-1}) is much greater than for Scilla (27 m s^{-1}), thus causing stronger impact and drag forces, and prompt deceleration of the block. The reason for the different behaviour is the steeper sloping angle for Albano: 42° on average in the

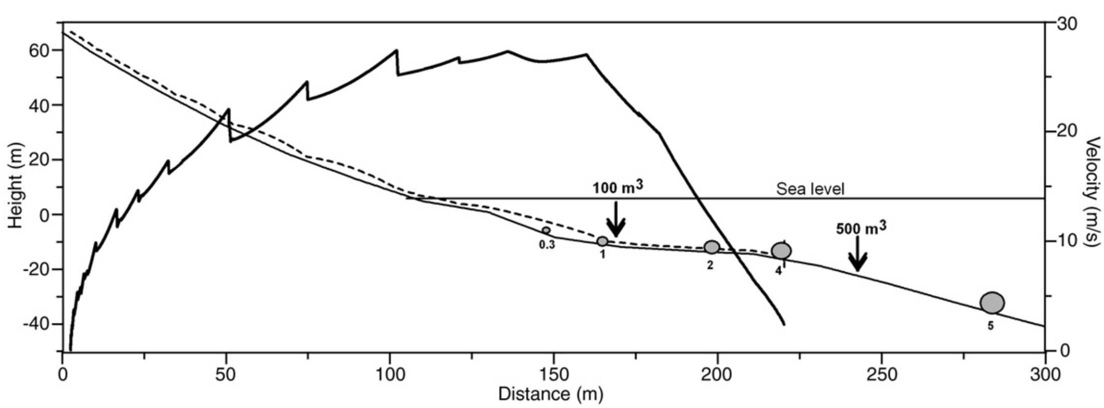

Fig. 3. Simulation of the block fall in the Scilla basin. The trajectory is for a block of radius 4 m. We also show the ending point of some smaller blocks; radiuses are reported near the block symbol. The position of real blocks found in the basin is indicated with circles, together with the estimated volume. The parameters used in the simulations are reported in Table 1. The velocity of the simulation corresponding to the 4 m block is also shown (solid line), superimposed to the trajectory (dashed line).

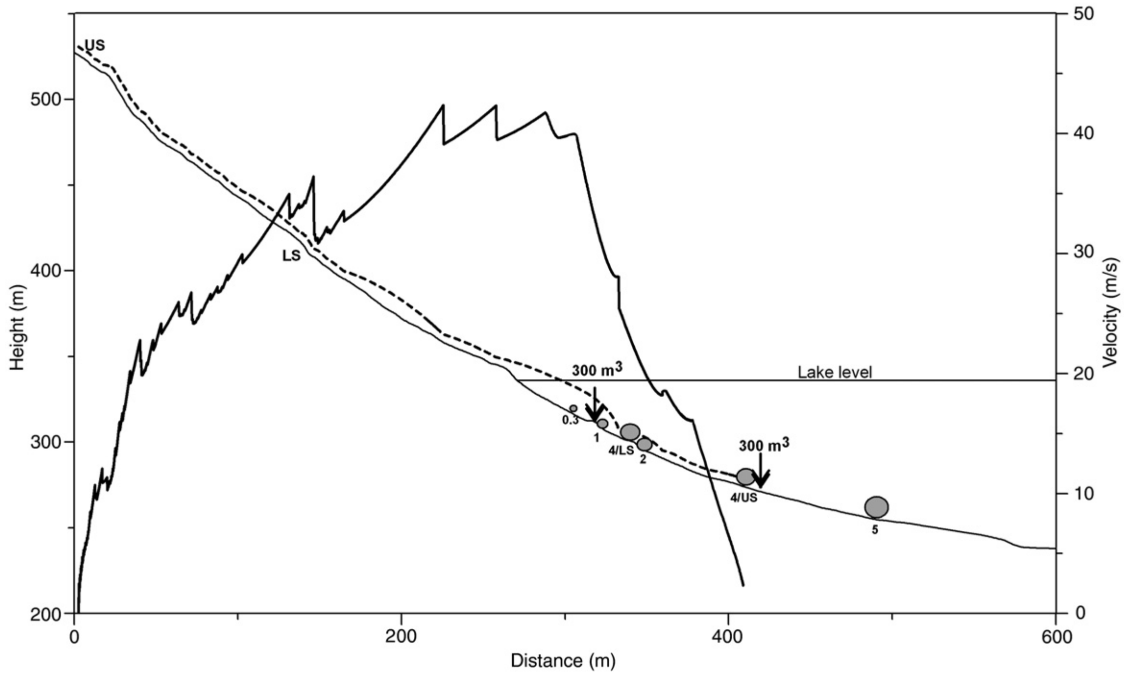

Fig. 4. Simulations for the Albano MRF. Symbols and numbers are common to Fig. 2. (US = Upper Scarp; LS = Lower Scarp).

subaerial part against 28° of Scilla, and 18° against 12° for the subaqueous environment. By running simulations with different block radii (circles), we found again a tendency of the run-out to decrease with decreasing block size. The case of Albano, however, poses an interesting challenge. The two blocks observed underwater (indicated with arrows in Fig. 4) have nearly the same size but a very different run-out, in apparent contradiction with the model. As for the Scilla MRF, the parameter set was chosen to reproduce the position of the block with longest run-out, though this resulted in a poorly predicted run-out for the other block. A possible explanation is that this block detached from a lower point. We thus made some simulations starting the block from a second, lower scar indicated as "LS" in Fig. 4 to distinguish it from the upper scar "US" used previously. The simulation clearly provides a much better similarity with data.

To assess the role of the water on blocks mobility, calculations were made in the absence of water (thus neglecting the impact force, buoyancy, and drag forces). Results indicate a run-out between 30% and 50% longer. Finally, we notice that the shape of the blocks observed underwater is poorly known. Although real rockfall blocks obviously depart from the ideal cylindrical shape used in the simulations, most subaerial rockfall blocks from the same area appear regular and sub-spherical.

4. Conclusions and outlook

We have introduced a model to describe and simulate the propagation of mixed subaerial–subaqueous rockfalls. We found that the presence of water is crucial in determining the block velocity and final run-out, as water develops a strong drag and impact resistance; in addition, lower normal restitution coefficients are expected in the submerged environment. The model predicts that the run-out increases as a function of block radius. This is because the drag force increases with the surface of the body, whereas the gravity pull is proportional to the volume. Although this is rather apparent in terms of basic physics, our model provides a framework to make this prediction more quantitative. Overall, we found a reasonable agreement between the run-out predicted by the theory and the position of the observed blocks. Based on the model results, we also suggest a significant dependence of the block run-out on the height of the detachment scarp.

A further analysis based on similar calculations may assist in identifying the most dangerous detachment zones; this is especially relevant when the slope ends directly into the water basin and direct data (lithology, geology, geometry) are not available so that the source of the block cannot be inferred.

The trajectory of a real block depends on the shape and details of the topography. In the simulations, we found that slightly shifting the initial trajectory of the block may result in significant differences of the final trajectory, even for the very regular blocks used here. In the field, divergences in the trajectories for blocks falling from the same height may result from small differences in the exact position of impact and on block size and shape. Thus, the spread resulting from the calculation is minor compared to the one observed in the field. However, these simple considerations apply equally well to the purely subaerial rockfall problem. Further inquiry should also assess the numerical values of the friction and restitution coefficients in subaerial and subaqueous environments, and their dependence on the block velocity. This will probably require experimental investigations. More subtle effects, such as block disintegration, should also be considered in a more complete treatment.

Due to the dependence on fine details and the use of a simple shape for the block, it is not sensible to seek for a precise correspondence between data and single simulations; block positions and velocities have more value in a statistical sense. It will be interesting to validate the present model by comparing more data with the numerical results of a statistical approach, where numerous block trajectories slightly different in the initial conditions are simulated rather than single events, and a statistical model for velocity and run-out is established.

Acknowledgements

We appreciate useful comments by the referee Jan Kalvoda, by one anonymous reviewer, and by the editor Takashi Oguchi.

References

Azzoni, A., De Freitas, H.M., 1995. Prediction of rockfall trajectories with the aid of in situ test. Rock Mechanics and Rock Engineering 28, 111–124.

Beranger, M., Carpaneto, R., Boote, D., Zucarelli, F., 1998. Probabilistic assessment of rockfall impact on subsea pipelines. OMAE 1998: Proceedings 17th International Conference on Offshore Mechanics and Arctic Engineering.
Bozzano, F., Gaeta, M., Martino, S., Mazzanti, P., Montagna, A., Prestininzi, A., 2008. The 1783 Scilla rock avalanche (Calabria, Southern Italy). In: Chen, M., et al. (Ed.), Proc. of the 10th Int. Symp. on Landslides and Engineered Slopes (30 June–04 July 2008) Xi'an, China, pp. 1381–1387.
Bozzano, F., Mazzanti, P., Anzidei, M., Esposito, C., Floris, M., Bianchi Fasani, G., Esposito, A., 2009. Slope dynamics of Lake Albano (Rome, Italy): insights from high resolution bathymetry. Earth Surface Processes and Landforms 34, 1469–1486.
Bozzolo, D., Pamini, R., 1986. Simulation of rock falls down a valley site. Acta Mechanica 63, 113–130.
Chiocci, F.L., Romagnoli, C., Tommasi, P., Bosman, A., 2008. The Stromboli 2002 tsunamigenic submarine slide: characteristics and possible failure mechanisms. Journal of Geophysical Research 113, B10102.
Clift, R., Grace, J.R., Weber, M.E., 1978. Bubbles, Drops, and Particles. Dover, Mineola.
Crosta, G.B., Frattini, P., Agliardi, M., Andreolli, M., Blikra, L.H., 2007. Modelling rockfall hazard in the Storfjorden area, western Norway. Geophysical Research Abstracts 9, 06437.
De Blasio, F.V., Sæter, M.-B., 2009. Rolling friction on a granular medium. Physical Review. E, Statistical Physics, Plasmas, Fluids, and Related Interdisciplinary Topics 79, 022301.
Dorren, L.K.A., 2003. A review of rockfall mechanics and modelling approaches. Progress in Physical Geography 27, 69–87.
Evans, S.G., Hungr, O., 1993. The assessment of rockfall hazard at the base of talus slopes. Canadian Geotechnical Journal 30, 620–636.
Giani, G.P., 1992. Rock Slope Stability Analysis. Balkema, Rotterdam.
Goldsmith, W., 1960. Impact. Dover, New York.
Gondret, P., Lance, M., Petit, L., 2002. Bouncing motion of spherical particles in fluids. Physics of Fluids 14, 643–652.
Guzzetti, F., Crosta, G.B., Detti, R., Agliardi, F., 2002. STONE: a computer program for the three-dimensional simulation of rock-falls. Computers & Geosciences 28, 1079–1093.
Harbitz, C.B., Pedersen, G., Gjevik, B., 1993. Numerical simulation of large water waves due to landslides. Journal of Hydraulic Engineering 119, 1325–1342.
Hughes, W.F., Brighton, J.A., 1967. Fluid Dynamics. McGraw Hill, New York.
Jones, C.L., Higgins, J.D., Andrew, R.D., 2000. Colorado Rockfall Simulation Program Version 4.0. Colorado Department of Transportation. Colorado Geological Survey.
Joseph, G.G., Zenit, R., Hunt, M.L., Rosenwinkel, A.M., 2001. Particle-wall collisions in a viscous fluid. Journal of Fluid Mechanics 433, 329–346.
Longva, O., Janbu, N., Blikra, L.H., Bøe, R., 2003. The 1996 Finneidfjord slide; seafloor failure and slide dynamics. In: Locat, J., Mienert, J. (Eds.), Submarine Mass Movements and their Consequences, 1st International Symposium. Kluver Academic Publishers, Dordrecht, pp. 531–538.
Mazzanti, P., Bozzano, F., Esposito, C., 2007. Submerged landslides morphologies in the Albano Lake (Rome, Italy). In: Lykousis, V., Sakellariou, D., Locat, J. (Eds.), Proceedings of 3rd International Symposium "Submarine Mass Movements and Their Consequences". Series: Advances in Natural and Technological Hazards Research, 27. Springer, Heidelberg, pp. 243–250.
Mazzanti, P., 2008. Analysis and modelling of coastal landslides and induced tsunamis. Ph. D. Thesis, Department of Earth Sciences, "Sapienza" University of Rome.
Miller, D.J., 1960. Giant waves in Lituya Bay, Alaska. U.S. Geological Survey Professional Paper 354-C, 51–84.
Moghisi, M., Squire, P.T., 1981. An experimental investigation of the initial force of impact on a sphere striking a liquid surface. Journal of Fluid Mechanics 108, 133–146.
Pfeiffer, T., Bowen, T., 1989. Computer simulation of rockfalls. Bulletin of the Association of Engineering Geologists XXVI (1), 185–196.
Shiffman, M., Spencer, D.C., 1945. The force of impact on a sphere striking a water surface. Approximation by the Flow about a Lens. Applied Math. Panel, National Defense Research Committee, Report No. 105.
Turmel, D., Locat, J., 2007. Underwater rockfall kinematics: a preliminary analysis. In: Lykousis, V., Sakellariou, D., Locat, J. (Eds.), Submarine Mass Movement and Their Consequence. Kluwer Academic Publishers, Dordrecht, pp. 139–147.